

Electrical and optical properties of spin-coated SnO₂ nanofilms*

WERONIKA IZYDORCZYK^{1†}, KRZYSZTOF WACZYŃSKI¹, JACEK IZYDORCZYK¹,
PAWEŁ KARASIŃSKI², JANUSZ MAZURKIEWICZ³, MIROŚLAW MAGNUSKI¹, JERZY ULJANOW¹,
NATALIA WACZYŃSKA NIEMIEC¹, WOJCIECH FILIPOWSKI¹

¹Silesian University of Technology, Institute of Electronics, Akademicka 16, 44-100 Gliwice, Poland

²Silesian University of Technology, Dept. of Optoelectronics, B. Krzywoustego 2, 44-100 Gliwice, Poland

³Silesian University of Technology, Institute of Engineering Materials and Biomaterials,
S. Konarskiego 18, 44-100 Gliwice, Poland

SnO₂ nanocrystalline thin films have been deposited on oxidized silicon substrates by spin-coating from a precursor solution, followed by slow thermal annealing in oxygen atmosphere at different temperatures (500 to 900 °C). The precursor solution consisted of 1.0 to 2.0 M SnCl₄·5H₂O in isopropanol. It was shown that the concentration of the precursor solution, annealing temperature and heating rate had a significant effect on the structural, optical and electrical properties of the studied thin films. The topography of SnO₂ thin films was examined by scanning electron microscopy (SEM). Furthermore, as-deposited films were characterized by X-ray diffraction (XRD), UV-Vis and impedance spectroscopy.

Keywords: *spin-coating; tin dioxide; UV-Vis spectroscopy; X-ray diffraction*

© Wrocław University of Technology.

1. Introduction

Tin dioxide is a direct transition wide band gap n-type semiconductor ($E_g = 3.6$ eV at 300 K) with a tetragonal crystal structure. SnO₂, due to its unique properties, has been widely used for gas sensing, various photocatalytic applications, such as optical coatings and liquid crystal displays [1–5]. Indium tin dioxide (ITO) and antimony-doped tin dioxide (ATO) are used as anode material in organic light emitting diodes (OLEDs) [6]. Tin dioxide layers doped with antimony or iron ions are used in electroluminescent devices [6, 7]. Doping a small amount of a transition metal (Fe, Cr, Co, Ni, V) into non-magnetic oxides could induce room temperature ferromagnetism, indicating the potential of such systems for spintronic applications [8–16]. Combinations of various

semiconductors (SnO₂, TiO₂, ZnO) and noble metals (Ag, Au, Pd and Pt) boost photocatalytic activity by trapping photo-induced charge-carriers and improving charge transfer process [1–3, 15, 16]. Such semiconductor-metal composite films have potential applications in improving the performance of photoelectrochemical solar cells [6]. Ag doped ITO nanofilms can be used to design antireflection coating systems [16].

Nanometer scale metals show special light absorption properties if they are smaller than incident light wavelength (Surface Plasmon Resonance – SPR). Metallic nanostructures can produce strong light absorption at a specific wavelength. It can be attributed to the localized surface plasmon oscillations of electrons in metal nanoparticles that are excited by light. Localized SPRs of metal nanoparticles are also affected by their sizes and shapes. Au and Ag nanoparticles are the most popular plasmonic nanoparticles. SPR electron transfer from the metal surface to adjacent semiconductor vastly alter optical properties of both materials.

*This paper was presented at the 37th International Microelectronics and Packaging IMAPS-CPMT Poland Conference, September 22 – 25, 2013, Kraków.

[†]E-mail: Weronika.Izydorczyk@polsl.pl

The band gap energy decreases with noble metal content [17, 18].

The aim of this work was to study the effect of annealing temperature and molar concentration of tin (IV) chloride pentahydrate solution in isopropanol on the structural and optical properties of SnO₂ thin films. Examined thin films were prepared by spin-coating method on silicon and quartz substrates, previously covered with a thin layer of gold. The authors also proposed an equivalent circuit for one of the films. Prepared SnO₂/Au nanolayers may find applications in gas sensors.

2. Experimental

Homogeneous layers of tin dioxide were formed by spin-coating a mixture of 1M, 1.5M and 2M of SnCl₄·5H₂O and isopropanol on clean silicon surfaces covered by a thermal oxide layer and onto quartz, formerly covered with approximately 8 nm gold film. It occurred, that the thin film of gold greatly improved the stability, adhesion to the substrate and thin film homogeneity. The rotation speed was set at 2000 rpm. The samples were transported to a quartz chamber of a furnace and heated up to 150 °C for 10 minutes and then heated in oxygen atmosphere for 1 hour, at 500, 700 and 900 °C. Temperature changes were slow (10 °C/min) in order to limit tension in the surface and cracking. Oxygen flow rate was 1 dm³/min.

The qualitative X-ray phase analysis was carried out with an X-ray diffractometer (X'Pert PANalytical) using an X-ray lamp equipped with a Co anode at a wavelength of $\lambda = 1.78901 \text{ \AA}$, voltage of 40 kV, filament current of 30 mA and 2Θ range of 20 to 110°.

The topography of SnO₂/Au films formed on the quartz and SiO₂/Si substrates was investigated at 5 to 20 kV accelerating voltage by means of ZEISS SUPRA 25 high-resolution scanning electron microscope.

The measuring system (Fig. 1) that was used to measure the impedance of the samples as a function of frequency and the calculation algorithm were presented in our previous work [19]. The main part of the measuring system is

HP 85046A S-Parameter Test Set, which operates with HP 8753 Network Analyzer manufactured by Hewlett Packard. The frequency measuring range of the instrument is 300 kHz to 3 GHz. Sample measurements were made using a probe based on N-type angle connector and 50 Ω coaxial cable. The frequency dependence of the impedance was approximated by a rational function with the constraints on circuit described by the function [19]. Transmittance spectroscopy study in the spectral range of 200 to 1000 nm was performed with the application of UV-Vis HR4000CG (Ocean Optics) spectrophotometer.

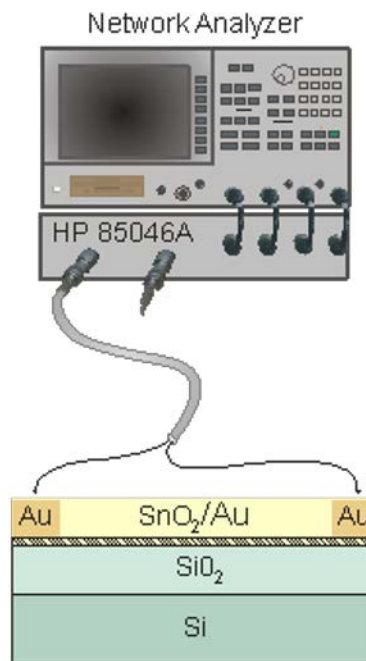


Fig. 1. System used for measurement of sample impedance.

3. Results and discussion

The results of the qualitative X-ray phase analysis revealed that the SnO₂ film was deposited on Au/SiO₂/Si substrate (Fig. 2), which has been proven by the identification of reflexes originating from crystallographic planes (110), (101), (200), (211), (112) and (321). These reflections can be attributed to tin dioxide with a tetragonal crystal structure (JCPDS 41-1445). Au reflexes originating from planes (111), (200), (202) and (311) were

identified (JCPDS Card No. 04-0784; cubic crystal structure).

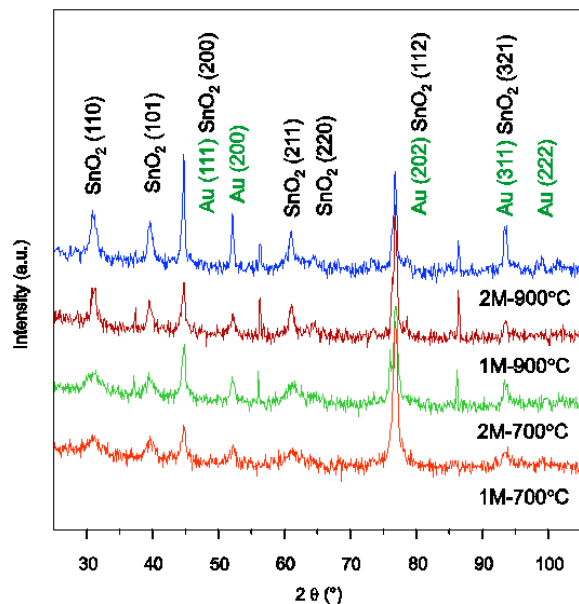


Fig. 2. XRD pattern of SnO₂/Au film formed on SiO₂/Si substrate and annealed at 700 and 900 °C, for two different molar concentrations of the precursor solution: 1M of and 2M of SnCl₄·5H₂O

Remaining reflexes originate from the substrate. There are no reflexes derived from other chemical compounds. The high intensity of the peaks indicates that these thin films primarily consist of a crystalline phase. The intensities of the SnO₂ (110) and Au (200) peaks are found to vary with the different molar concentrations of the precursor solution. The average size of the SnO₂ and Au nanoparticles was calculated using Debye-Scherrer formula. As shown in Table 1, the average size of SnO₂ crystallites formed at a temperature of 500, 700 and 900 °C are 5.1, 6.7, 12.9 nm, respectively, for 2M of SnCl₄·5H₂O solution.

Fig. 3a depicts SEM images of SnO₂ nano-layer after spin-coating of 2M SnCl₄·5H₂O solution in isopropanol on Au/SiO₂/Si and heating it up to 700 °C. SEM analysis shows that the surface is tightly and homogeneously covered with nanoparticles, whose dimensions vary in 17 to 27 nm range, and which accumulate into bigger agglomerates of elongated shapes. In comparison, the

layer obtained by spin-coating of 2M solution and heated up to 900 °C, reveals similar surface morphology but the observed structures contain larger nanoparticles, about 30 to 46 nm in diameter (Fig. 3b). Author of [20] also noted that the SnO₂ nanoparticles show a tendency to grow with increasing annealing temperature. Glancing-Incidence XRD research done by authors [4] showed that SnO₂ layers heated up to 350 °C, are amorphous.

Size of nanocrystallites, formed in amorphous tin oxide layer depends on oxide atmosphere, heating process temperature as well as on tin tetrachloride molar concentration in isopropanol. In the 350 to 500 °C temperature range crystallites grow slowly, their diameter does not exceed 5 nm.

SEM image analysis depicting the surface of SnO₂ thin film formed at various annealing temperatures, and in an oxygen atmosphere, shows that as the temperature increases from 500 °C, the number of crystallites, and the diameter of nanograins rapidly increases [4].

The absolute value and phase of impedance of the sample, measured directly with HP 85046A S-Parameter Test Set, which operated with HP 8753 Network Analyzer in the frequency range of 0.3 to 20 MHz, are presented in Fig. 4a and 4b. The normalized measurement data were approximated by a rational function, with order N equal to the number of measurement points/frequencies. The function is expressed as a series of partial fractions: $Z(\omega) = \sum_i (c_i / (j\omega - p_i))$. As the approximating function is a function of high degree, the measurement data are reproduced with very high accuracy. The function, however, consists of a few major components, and the whole swarm of minor components. The authors assume that the minor components are needed to reproduce the measurement errors, whereas the major components are associated with the equivalent circuit of the sample. The criterion for distinguishing the major components from the minor ones is the absolute value of the residue of the component, $|c_i|$. As a result, the equivalent circuit, depicted in Fig. 4d, includes only those components of the series, which (1) have the largest absolute value of the residuum $|c_i|$; (2)

Table 1. Full width at half maximum (FWHM) of the SnO₂ (110) and Au (200) peaks and the corresponding crystallite sizes (calculated using Debye-Scherrer formula) for SnO₂/Au layers formed at various temperatures (500, 700 and 900 °C) and molar concentrations of SnCl₄·5H₂O.

Molar concentration of the precursor solution and annealing temperature	FWHM values of the SnO ₂ (110) peak (°)	SnO ₂ crystallite size (nm)	FWHM values of the Au (110) peak (°)	Au crystallite size (nm)
2.0 M-500 °C	1.89	5.1	0.63	16.7
1.0 M-700 °C	1.47	6.6	0.71	14.9
1.5 M-700 °C	1.46	6.6	0.55	19.4
2.0 M-700 °C	1.45	6.7	0.53	20.0
1.0 M-900 °C	0.88	11.1	0.52	20.7
1.5 M-900 °C	0.85	11.5	0.50	21.5
2.0 M-900 °C	0.76	12.9	0.39	27.4

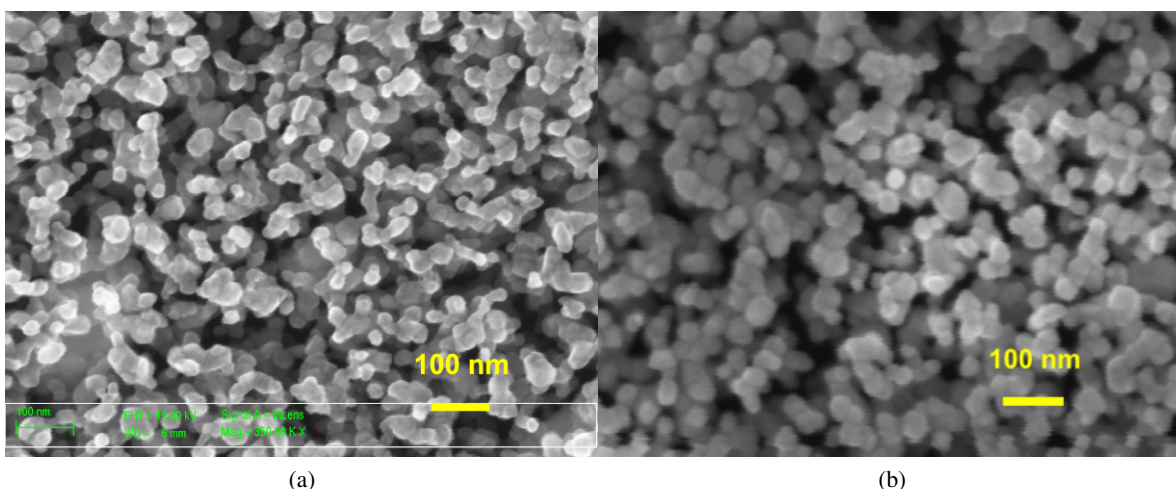


Fig. 3. SEM images of SnO₂/Au film formed on SiO₂/Si substrate and annealed at (a) 700 and (b) 900 °C.

pole $|p_i|$ lies on the left half-plane; (3) for the complex conjugate pole pair, Foster passivity condition is satisfied. The impedance measurement results were compared with the input impedance of the equivalent circuit, as shown in Fig. 4a–4c. The circuit impedance was calculated using LTSpice simulator. Consistency of the measurement data and calculations was found to be excellent.

Methodology used by the authors to identify equivalent circuit parameters of the sensor allowed us to indicate, which of the two hypotheses on the meaning of each RC section is more likely. In literature one could find a commonly accepted

opinion that the RC model of a tin dioxide sensor consists of three cascaded circuits [21–25]. The first circuit consists of a resistance only. It is the resistance of the bulk tin dioxide. The author of [23] does not exclude that, in fact, this circuit is a parallel RC circuit but the time constant of this circuit is impossible to measure if the impedance measurements are performed at frequencies $\nu < 1$ MHz. The time constant of this circuit is then associated with the processes of generation and recombination of carriers in the semiconductor volume. In the case of the sensor described in this article, bulk resistance of the semiconductor can be associated with the circuit R₅C₅, whose cut-off frequency

$\nu_5 = 1/(2\pi R_5C_5)$ is above 500 MHz. A second RC circuit that is described in the literature, relates to the Schottky junction, which is formed between the metal connector and the semiconductor. In the case described here, the sensor connectors are made of gold. The work function (5.51 eV) of gold is higher than the work function of tin dioxide (4.7 eV). As a result, under the connectors, a Schottky junction is formed. This circuit may be identified with the R_1C_1 circuit in Fig. 4d. Circuit R_1C_1 has a cut-off frequency $\nu_1 = 14.4$ MHz, which is a very probable value for the Schottky connection with such a large area. The third circuit known from the literature consists of a resistance and a constant phase element (CPE). Impedance of a CPE is equal to $1/(j \cdot \omega^n)$, where n varies depending on the sensor, from 0.74 [23] to 0.97 [25]. In the literature, there is a consensus that this circuit describes the dynamics of the transport and accumulation of charge on single crystal grain boundaries, in particular, on the border of nanowires. However, the author of [22] justifies the need for a CPE element whose particle size of single crystals take the values from a continuous range in the real sensor, which corresponds to a swarm of RC circuits with different cut-off frequencies. Meanwhile, the analysis carried out by the authors of this article indicates that there is no such a phenomenon. A swarm of RC circuits can be attributed to measurement uncertainty rather, as the swarm includes only small number (namely three) RC circuits, which seem to be essential. They shape the impedance of the sensor at low frequencies. This confirms the thesis of the author of [23] that the migration of charged particles on the surface of a single crystal is responsible for the CPE element. Author [23] had in mind the ions O_2^- , O^- , OH^- adsorbed on the monocrystal surface or a defect V_O^{2+} in the bulk of semiconductor. The authors of this publication managed to decompose the CPE into three RC circuits with a cut-off frequencies $\nu_2 = 1.65$ MHz, $\nu_4 = 534$ kHz and $\nu_3 = 38.1$ kHz, respectively.

Final confirmation of this hypothesis requires a measurement of the impedance of the sensor for different frequencies, different temperatures and in the presence of different gases: as oxidizing

and reducing agents. Carrying out these measurements requires troublesome high frequency measurements connected with the measurements in a flow chamber at high temperature. The authors are just designing such measurements.

The UV-Vis transmission spectra of the SnO₂/Au films formed on quartz by spin-coating are shown in Fig. 5a and 5b. Pure SnO₂ films (Fig. 5b – sample 500-SnO₂) are highly transparent in the region above 400 nm, which is the region of interest for electro-optical devices [7]. As can be seen SnO₂/Au layers may absorb in UV as well as in the visible light spectrum. On the other hand, it is evident that the optical transmission of SnO₂/Au films in the visible region has improved with increasing annealing temperature due to improved crystallinity of SnO₂ nanoparticles.

The formation of gold nanoparticles during the process of annealing can be confirmed by the appearance of characteristic plasmon minima at 532, 542 and 536 nm in the transmittance spectrum for samples Au-500, Au-700 and Au-900, respectively (Fig. 5a). A red shift with respect to the plasmon resonance peak of gold (550, 553 and 548 nm for samples formed from 1.5M of SnCl₄·5H₂O solution at temperature of 500, 700 and 900 °C) and broadening of the plasmon band are observed in SnO₂/Au films (Fig. 5a and 5b). Corresponding plasmon peak at 583 nm was obtained in the transmittance spectrum for the sample with a higher initial thickness of gold layer $d_{Au} = 16.5$ nm (Fig. 5a).

The observed red shift in the LSPR spectra is due to the increase in size of gold nanoparticles [26] and agglomeration of gold nanoparticles [2], which is accompanied by changes in materials and chemical properties. In addition, the plasmon bandwidth at half maximum increases with the size of gold nanoparticles (diameter larger than 22 nm) [26]. On the other hand, interfacial as well as inter-particle interactions are also a significant cause of red-shift and broadening of the plasmon band of the Au nanoparticles.

In order to determine the optical band gap energy of the SnO₂/Au nanofilms, the absorption coefficient α of the film was evaluated from the

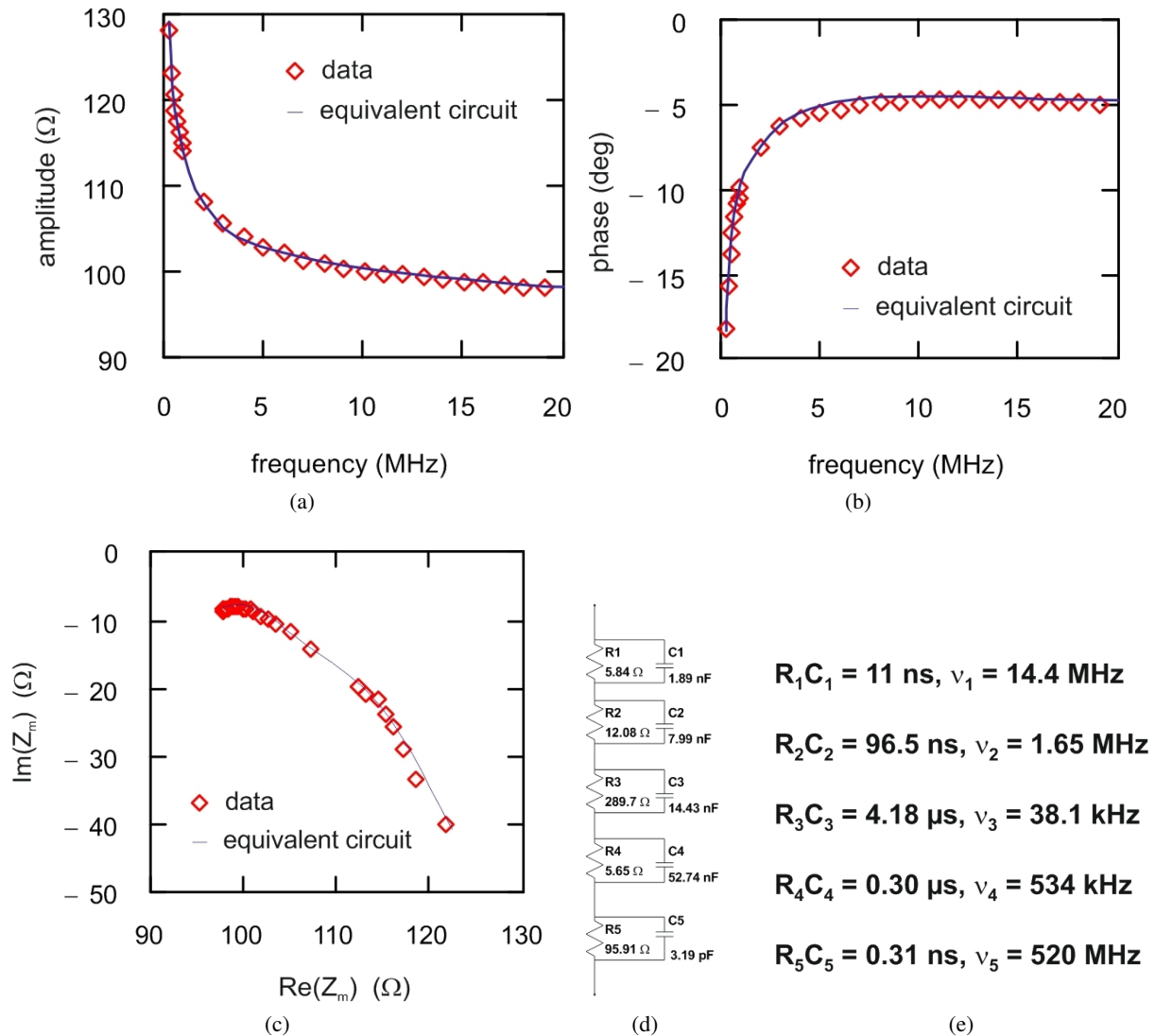


Fig. 4. Results of measuring the absolute value (a) and phase (b) of impedance of SnO₂/Au film (2M, 900 °C), comparison of the measured impedance and the impedance calculated on the basis of the equivalent circuit using a SPICE simulator (c), equivalent circuit (d), calculated RC constants and cut-off frequencies (e).

transmittance T spectra of the nanofilm and its thickness d [27]:

$$\alpha = -\frac{\ln(T)}{d} \quad (1)$$

The optical band gap E_g (related to direct transition) in SnO₂ film was determined using the Tauc's relationship [28]:

$$\alpha h\nu = A(h\nu - E_g)^{\frac{1}{2}} \quad (2)$$

α – absorption coefficient, $h\nu$ – photon energy, A – constant.

Fig. 5b. shows the dependence of $(\alpha h\nu)^2$ as a function of photon energy $h\nu$. The band gap was determined by extrapolating the straight line portion of the graph to the photon energy axis. It is seen that for SnO₂/Au films a lower optical band gap ($E_g = 3.83 \text{ eV}$) could be obtained by increasing the initial thickness of the gold layer ($d_{\text{Au}} = 16.5 \text{ nm}$) and annealing temperature (1.5 M solution, 900 °C). Average SnO₂ nanoparticle size increases from 22 to 38 nm with the increase in the annealing temperature from 700 to 900 °C. The corresponding values of optical band gaps obtained

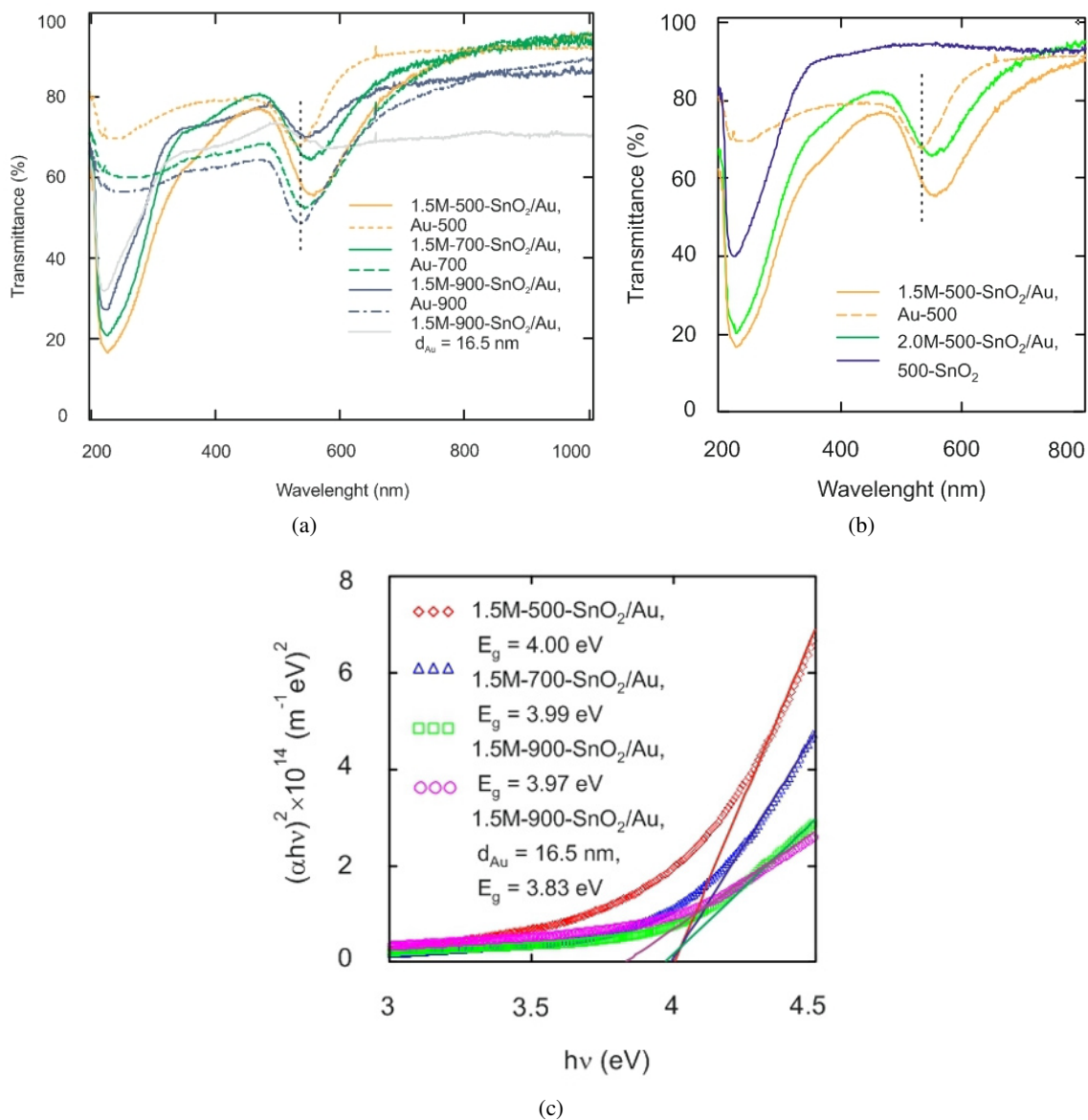


Fig. 5. Optical properties of the SnO₂ and SnO₂/Au films formed on quartz and annealed at 500, 700 and 900 °C. (a), transmittance spectra (b), plot of $(\alpha h\nu)^2$ vs. $h\nu$, (c) – determination of optical band gap energy from UV absorption spectra.

from the calculations: 3.99 and 3.97 eV, are larger than the value of 3.6 eV of the bulk of SnO₂ [7].

4. Conclusions

The results of the qualitative X-ray phase analysis revealed that the SnO₂ thin film was deposited on Au/SiO₂/Si substrate. SEM analysis showed that the grains had a tendency to grow in size with

increasing annealing temperature. Equivalent circuit was used for analysis of the impedance plots.

In the transmittance spectra, the minima related to the surface plasmon resonance of the Au nanoparticles were observed. It was shown that for SnO₂/Au films a lower optical band gap could be obtained by increasing the initial thickness of the gold layer and annealing temperature.

References

- [1] BAJAJ G., SONI R.K., *Open Surf. Sci. J.*, 3 (2011), 65.
- [2] TARWAL N.L., DEVAN R.S., MA Y.R., PATIL P.S., *Electrochim. Acta*, (2010), DOI:10.1016/J.ELECTACTA.2012.03.135.
- [3] GAIDI M., HAJJAJI A., SMIRANI R., BESSAIS B., EL KHAKANI M.A., *J. Appl. Phys.*, 108 063537 (2010), 1.
- [4] BAZARGAN S., HEINIG N.F., PRADHAN D., LEUNG K.T., *Cryst. Growth Des.*, 11 (2011), 247.
- [5] BADALYAN S.M., RUMYANTSEVA M.N., NIKOLAEV S.A., MARIKUTSA A.V., SMIRNOV V.V., ALIKHANIAN A.S., GASKOV A.M., *Inorg. Mater.*, 46 (2010), 232.
- [6] LUO L., BOZYIGIT D., WOOD V., NIEDERBERGER M., *Chem. Mater.*, 25 (2013), 4901.
- [7] SHARMA S., VOLOSIN A.M., SCHMITT D., SEO D.-K., *J. Mater. Chem. A*, 1 (2013), 699.
- [8] HOA HONG N., SAKAI J., PRELLIER W., HASSINI A., *J. Phys.-Condens. Mat.*, 17 (2005), 1697.
- [9] PAN F., SONG C., LIU X.J., YANG Y.C., ZENG F., *Mater. Sci. Eng. R-Rep.*, 62 (2008) 1.
- [10] COEY J.M.D., DOUVALIS A.P., FITZGERALD C.B., VENKATESAN M., *Appl. Phys. Lett.*, 84 (2004), 1332.
- [11] LIU X.F., SUN Y., YU R.H., *J. Appl. Phys.*, 101 (2007), 123907.
- [12] WANG X.L., ZENG Z., ZHENG X.H., *J. Appl. Phys.*, 101 (2007), 09H104.
- [13] OGALE S.B., CHOUDHARY R.J., BUBAN J.P., LOFLAND S.E., SHINDE S.R., KALE S.N., KULKARNI V.N., HIGGINS J., LANCI C., SIMPSON J.R., BROWNING N.D., DAS SARMA S., DREW H.D., GREENE R.L., VENKATESAN T., *Phys. Rev. Lett.*, 91 (2003), 077205.
- [14] BORGES P.D., SCOLFARO L.M.R., LEITE ALVES H.W., DA SILVA JR. E.F., ASSALI L.V.C., *Nanoscale Res. Lett.*, 7 (2012), 540.
- [15] PAWLICKA A., *Recent Pat. Nanotech.*, 3 (2009), 177.
- [16] CHUN-BIN C., LEI X., XUE-PING S., ZHAO-QI S., *J. Vac. Sci. Technol. A*, 28 (2010), 48.
- [17] GULLIEN C., HERRERO J., *J. Phys. D Appl. Phys.*, 46 (2013), 295302.
- [18] GASPAR D., PIMENTE A.C. MATEUS T., LEITA J.P., SOARES J., FALCA B.P., ARAUJO A., VICENTE A., FILONOVICH S.A., A'GUAS H., MARTINS R., FERREIRA I., *Sci. Rep.-UK*, 3 (2013), 1469.
- [19] IZYDORCZYK W., IZYDORCZYK J., MAZURKIEWICZ J., MAGNUSKI M., ULJANOW J., *Electrical characterization of 1D SnO₂ nanowires, 12th IEEE Conference on Nanotechnology. NANO'12*, Birmingham, United Kingdom, 20 – 23 August 2012, 1 – 6.
- [20] MAJUMDER S., *Mater. Sci.-Poland*, 27 (2009), 123.
- [21] FIERRO L.G. (Ed.), *Metal Oxides: Chemistry and Applications*, CRC Taylor & Francis, Boca Raton, 2006.
- [22] WEIMAR U., *Gas Sensing with Tin Oxide: Elementary Steps and Signal Transduction*, University of Tübingen, 2001.
- [23] SCHIERBAUM K.-D., *Sensor. Actuat. B-Chem.*, 24 – 25 (1995), 239.
- [24] SCHMID W., *Consumption measurements on SnO₂ sensors in low and normal oxygen concentration*, University of Tübingen, 2004.
- [25] HERNÁNDEZ-RAMÍRES F., TARANCÓN A., CASALS O., RODRÍGUEZ J., ROMANO-RODRÍGUEZ A., MORANTE J.R., BARTH S., MATHUR S., CHOI T.Y., POULIKAKOS D., CALLEGARI V., NELLEN P.M., *Nanotechnology*, 17 (2006), 5577.
- [26] LINK S., A. EL-SAVED M., *J. Phys. Chem. B*, 103 (1999), 4212.
- [27] KARASIŃSKI P., GONDEK E., DREWNIAK S., KITYK I. V., *J. Sol-Gel Sci. Techn.*, 61, (2012), 355.
- [28] TAUC J., GRIGOROVICI R., VANCU A., *Phys. Status Solidi A*, 15 (1966), 627.

Received 2014-01-13
Accepted 2014-10-14